



CrossMark  
 click for updates

Cite this: *RSC Adv.*, 2015, 5, 29947

Received 15th February 2015  
 Accepted 20th March 2015

DOI: 10.1039/c5ra02928g

[www.rsc.org/advances](http://www.rsc.org/advances)

# Stability of molecular layer deposited zincone films: experimental and theoretical exploration†

Devika Choudhury,<sup>a</sup> Gopalan Rajaraman<sup>b</sup> and Shaibal K. Sarkar<sup>\*a</sup>

The degradation mechanism of MLD grown hybrid organic inorganic materials under ambient atmosphere is investigated with zincone as the material of study. Time dependent Fourier transform infrared (FTIR) spectroscopy is used to analyze the chemical changes in the material. Experimental findings are well supported by theoretical study using Density Functional Theory (DFT) calculations.

## Introduction

A growing interest is discernible in hybrid materials in recent years due to the enormous potential of combining the characteristic properties of their organic and inorganic constituents, resulting in new materials with tunable physical, chemical and electronic properties.<sup>1–4</sup> These hybrid materials have found promising applications in various domains, such as barrier layers, encapsulants *etc.*<sup>5–8</sup> Lately, applicability of these materials in (opto)electronics<sup>9–11</sup> is also being explored. Recently Yoon *et al.* studied thin films of a blend of organic molecules and zinc oxide that offered tunability in electronic properties.<sup>12</sup> This seeds the probable scope to explore the use of hybrid organic inorganic materials as transparent and flexible electronics in future.

Various deposition techniques like chemical vapour deposition (CVD),<sup>13,14</sup> spin coating method,<sup>15</sup> Langmuir–Blodgett method,<sup>16,17</sup> self assembly technique<sup>18</sup> are utilized to grow different hybrid thin films. The deposition of such films, however, has received a major boost after the realization of atomic layer deposition (ALD) and subsequently molecular layer deposition (MLD) techniques.<sup>19,20</sup> The ALD/MLD technique circumvents major drawbacks of the other methods with its capability of depositing uniform and conformal thin films with molecular level of thickness precision and control.<sup>21</sup> This has led to the growth of a variety of thin films by ALD/MLD using different combinations of organic and inorganic constituents in them.<sup>1</sup>

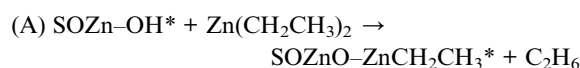
The most widely developed hybrid films by MLD are the “metalcones”, grown using a combination of different inorganic metalorganic precursors and organic reactants.<sup>2</sup> “Alucone” consisting of trimethylaluminum and ethylene glycol is one of the first metalcone film reported.<sup>22</sup> Similarly, “zincone” using diethylzinc (DEZ) and ethylene glycol (EG) is the first of such a zinc based hybrid metalcone film.<sup>23</sup> Various other materials like zircone,<sup>24</sup> titanicone<sup>25</sup> *etc.* have also been developed of late. However, most of these hybrid materials face two major constraints, lower growth rate<sup>22,23</sup> and instability in air.<sup>23,26–28</sup> Recently, homo/hetero bifunctional aromatic molecules are being used to replace the popularly used linear organic ones.<sup>29–31</sup> However, the rigidity of the aromatic compounds though provides structural stability to the materials, does not offer any permanent solution to the persisting chemical instability<sup>32</sup> of the hybrid films.

In this paper we elucidate the mechanism of degradation in organic inorganic hybrid materials. Here we consider zincone as the material under study. This study can be well extended to understand the generic stability concern of the MLD grown structures. The chemical deformation of the deposited films under ambient condition was studied by Fourier transform infrared (FTIR) spectroscopy that was complemented with theoretical studies based on Density Functional Theory (DFT) calculations.

## Experimental details

### Molecular layer deposition of zincone films

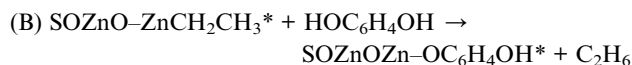
Molecular layer deposition was carried out in a laminar “flow type” custom built ALD reactor described elsewhere.<sup>32</sup> Self saturating surface chemistry with diethylzinc (DEZ, Sigma Aldrich) and hydroquinone (HQ, Sigma Aldrich) was used for the growth of zincone films at 150 °C. The zincone chemistry can be described by two half-surface chemical reactions as reported earlier,<sup>29</sup>



<sup>a</sup>Department of Energy Science and Engineering, Indian Institute of Technology Bombay, Mumbai-400076, India. E-mail: shaibal.sarkar@iitb.ac.in; Fax: +91 22 2576 4890; Tel: +91 22 2576 7846

<sup>b</sup>Department of Chemistry, Indian Institute of Technology Bombay, Mumbai-400076, India

† Electronic supplementary information (ESI) available: Additional FTIR spectra are presented. Optimized structures of zincone and hybrid structures with the related optimized energy obtained from DFT calculations are shown. See DOI: 10.1039/c5ra02928g



where \* denotes the surface species for reactions.

DEZ was kept at room temperature while HQ was heated to 130 °C with overhead N<sub>2</sub> flow arrangement for better vapour transport to the reactor. Controlled dosing of the precursors was obtained with adequate instrumentation operated with labview programming. Precursors were fed into the reactor through progressively heated channels. Each MLD cycle was composed of 1 second of DEZ pulse, 20 seconds of N<sub>2</sub> purge, 1 second of HQ pulse and again 20 seconds of N<sub>2</sub> purging. Thus the 1–20–1–20 time sequence was used for all film depositions. Films were grown under a constant base pressure of 0.9 Torr, maintained by 200 sccm of N<sub>2</sub> flow controlled with mass flow controller (MKS). N<sub>2</sub> was used both as the carrier gas and purging gas in this arrangement.

Resistance of the as deposited film was measured during deposition with an *in situ* resistance measurement under van der Paw configuration. Applying a constant current, the change in the resistance of the film was measured with time.

For *ex situ* FTIR spectroscopy studies, 300 MLD cycles of zincone was deposited on KBr pellets. Measurements were carried out in Vertex 70 instrument from Bruker equipped with both DTGS (deuterium triglyceride sulphate) and liquid N<sub>2</sub> cooled MCT (mercury doped cadmium telluride) detectors. The former was used to carry out measurements for zincone samples exposed to ambient. The latter was utilized to study the films when kept in vacuum. Absorbance spectra of the samples were obtained in the range of 4000 to 350 cm<sup>-1</sup> with a resolution of 4 cm<sup>-1</sup>. The spectrum obtained was averaged over 100 scans.

### Computational details

Theoretical analysis of the structure, bonding and energies of the zincone molecules was done by utilizing Density functional theory (DFT) calculations. For simplicity, gas phase models were used which closely resembled the reactants and products formed during the MLD process, thus considering infinite surrounding and neglecting steric hindrance between molecules as well as the effect of different substrates. Gaussian 03 program<sup>33</sup> was used to carry out all the calculations.

The geometries were optimized using hybrid B3LYP functional<sup>34,35</sup> and 6-31G\* basis set<sup>36</sup> for all the atoms. All the studied structures were fully optimized and frequency calculations were performed to verify their nature and also to obtain the IR spectra. All the reported energies are B3LYP/6-31G\* Gibb's free energy including zero-point, thermal and entropy corrections. DFT calculations were carried out at room temperature.

## Results and discussions

### Changes in electrical properties

The importance of zincone initially lies in the fact that the π–π\* orbitals of HQ molecules on reaction with DEZ might result in conjugated chains in the form of [(HO)Zn(OPhenylOH)]<sub>n</sub> thus making the zincone molecule electrically conductive.<sup>29</sup> However

the hypothesis was never overwhelmingly supported with experiments. Fig. 1(a) shows the *in situ* resistance measurements, using van der Paw technique during the pure zincone film growth of approx. 50 nm.

As seen clearly, the resistance of the film decreases with the increase in film thickness. The resistance becomes stable after ca. 40 nm of film deposition which is equivalent to approx. 250 MLD cycles of zincone film growth.<sup>32</sup> The decrease in resistance during deposition can be attributed to many possible phenomena namely surface or interface scattering, phonon scattering *etc.* either acting independently or additively.<sup>37</sup>

When exposed to air, an irreversible change in the resistance of zincone film was observed as shown in Fig. 1(b). However no observable change was noted when the film was kept under vacuum or under constant N<sub>2</sub> flow.

### Changes in the chemical nature of films

The irreversible change in resistance for zincone films could be possibly attributed to permanent chemical changes occurring within the zincone molecules on exposure of the as deposited film to ambient.

Time dependant FTIR spectroscopy measurements were carried out to investigate the changes (if any) in the chemical nature of the hybrid material. Films were deposited on KBr pellets and the spectra were recorded *ex situ* in ambient conditions over a time span of 48 hours initially. Theoretical calculations reproduced the obtained IR spectrum to confirm the assigned vibration stretches. Fig. 2 shows the FTIR spectra portraying the observed chemical signature of the deposited films. For clarity in presentation, the spectra have been shown from 1600 cm<sup>-1</sup> to 350 cm<sup>-1</sup> where the most prominent peaks lie.

The sharp absorbance peak observed at 1492 cm<sup>-1</sup> is due to the C=C stretching vibration of the aromatic ring present in HQ. In addition, C–O stretching vibration is observed at

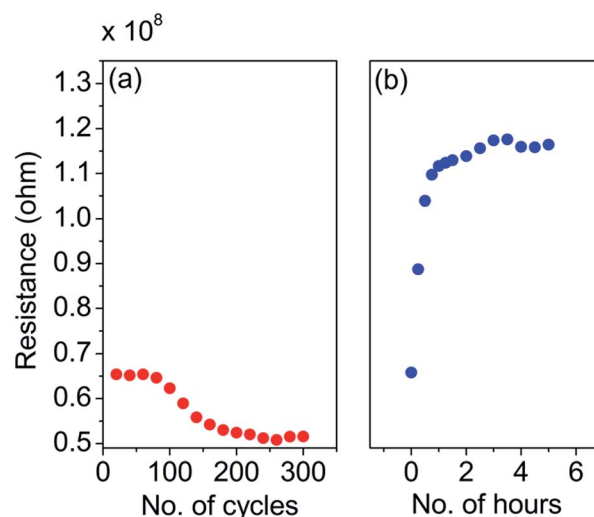


Fig. 1 *In situ* resistance measured (a) during deposition of zincone film, (b) during exposure to air.

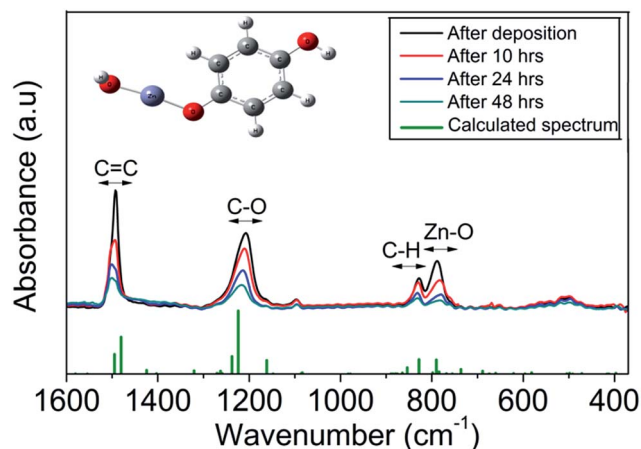


Fig. 2 FTIR spectra of 300 cycles of zincone film grown on KBr pellets and recorded over a time span of 48 hours. The sample under observation was exposed to ambient condition of 25 °C temperature and 60–70% humidity between each scan; spectrum of 2 MLD zincone cycles obtained from DFT calculations.

1205  $\text{cm}^{-1}$ . The third bifurcated peak at 827  $\text{cm}^{-1}$  and 788  $\text{cm}^{-1}$  can be attributed to the C–H vibration of the C–H bonds present in the aromatic ring of HQ and the Zn–O stretch from the Zn–O bond formed between DEZ and HQ<sup>23</sup> in the zincone molecule (shown in Fig. 2) respectively. As seen from Fig. 2 each of the signature peaks obtained in the FTIR spectra suffers a decrease in absorbance intensity with time, when exposed to air. This occurs with a simultaneous increase in the intensity of the O–H stretch (shown in Fig. SI-1 in ESI†). It is noteworthy here that no change of the signature peaks of zincone film is obtained when kept in vacuum for the same duration of time (shown in Fig. SI-2 in ESI†).

For closer inspection of the changes taking place, the as deposited zincone film was kept in ambient for a prolonged period of five days. A comparative study of the zincone film as deposited and after five days is shown in Fig. 3.

As seen from Fig. 3(a) and (b), there is a significant change in the peak positions of the spectra immediately after deposition of zincone and after five days. The single peak of C=C stretch at 1492  $\text{cm}^{-1}$  bifurcates into two at 1514  $\text{cm}^{-1}$  and 1473  $\text{cm}^{-1}$ . The presence of a new peak at 1367  $\text{cm}^{-1}$  is noteworthy here. Similarly the single peak corresponding to C–O at 1204  $\text{cm}^{-1}$ , disappears with the appearance of a bifurcated one with peaks at 1241  $\text{cm}^{-1}$  and 1216  $\text{cm}^{-1}$ . Moreover, though the C–H vibration peak at 827  $\text{cm}^{-1}$  remains, the Zn–O stretch at 788  $\text{cm}^{-1}$  disappears completely and a new peak appears at 757  $\text{cm}^{-1}$ . A new peak is also found at 520  $\text{cm}^{-1}$ . It was found that the entire spectrum of the zincone film obtained after prolonged exposure to ambient atmosphere closely resembles that of only HQ as shown in Fig. 3(c).<sup>38</sup> Table SI-1 in ESI† gives a detailed description of the different vibration stretches of HQ obtained from earlier reports and experimentally as well as the comparison of the HQ peak positions with the experimentally obtained FTIR spectrum of a zincone film after five days.

It is interesting to observe that the vibration stretch attributed to the Zn–O bond in the zincone molecule as seen in Fig. 3(a) disappears completely in Fig. 3(b). To investigate the degradation further, the bond length during zincone formation under stable state condition was calculated. A comparative study of the bond lengths, which in turn elucidates the bond energy, showed that the bond length of the Zn–Ophenyl in [Zn–Ophenyl(OH)] of zincone is highest and thus weakest among all possible bonds associated with Zn during the MLD growth, shown in Fig. 4. This drove to hypothesis that the degradation caused in the MLD grown zincone polymer results from cleavage of the labile chemical bond formed between Zn and the aromatic ring, depicted in Fig. 4.

The hypothesis is supported by the fact that the breakage of this Zn–O bond can explain the decrease of the Zn–O stretch at 788  $\text{cm}^{-1}$  observed experimentally in the FTIR spectra. This causes a decrease in the length of the zincone chains thus resulting in the simultaneous decrease in the intensities of the other signature vibration stretches.

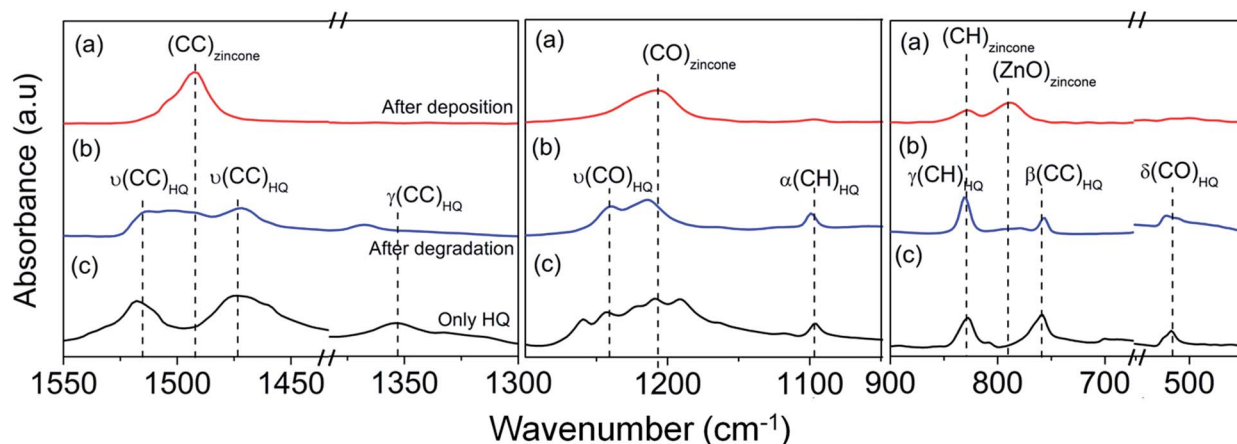
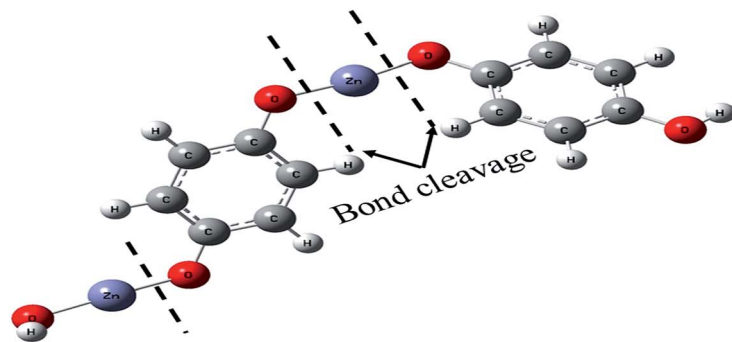


Fig. 3 FTIR spectra of zincone film deposited on KBr pellet (a) after deposition, (b) after prolonged exposure to ambient conditions compared with the FTIR spectrum of (c) only HQ.



Bond Name	Distance (Å)
Zn-OPhenyl	1.76
O-Phenyl	1.36
Zn-OH	1.74
Phenyl-OH	1.37

Fig. 4 Schematic showing the suspected breakage of Zn–O bond in [(HO)Zn(OPhenylOH)] resulting in the degradation of zincone film.

### Enhancing the stability of zincone films

As an effort to isolate the affect of the ambient, zincone films were capped with varied thicknesses of ALD grown ZnO films. All depositions were carried out in the same reactor without breaking the vacuum. It was found that *ca.* 20 nm of the ZnO capping makes the as deposited zincone films stable under the ambient condition as studied by FTIR with no degradation found within the experimental time frame (shown in Fig. SI-3 in ESI<sup>†</sup>). Earlier reports suggest that similar capping reduces moisture penetration from the atmosphere into the material thus preventing degradation.<sup>22</sup>

As already been mentioned and confirmed, the bond strength of the Zn–O in [Zn(OPhenyl(OH))] species is weak and can cleave under ambient conditions. Apart from the above solution of capping the films, insertion of the O–Zn–O moiety in the chain is also found to enhance the stability of the hybrid zincone film. The additional ZnO unit strengthens the Zn–O bond in [Zn–OPhenyl(OH)] species (shown in Fig. SI-4 in ESI<sup>†</sup>) resulting in a longer and stable chain formation. Experimentation supports the theoretical observation that incorporation of ten or more monolayer of zinc oxide resulted in stable hybrid film formation. This can be

depicted by the constant absorbance intensity of the Zn–O peak as shown in Fig. 5.

To further understand the atomistic structure and stability of the layer formations of zincone, theoretical investigations were performed to probe the thermodynamic stability and formation of the zincone molecular chains. The computed energetics of each of the half cycle reactions for the deposition of pure zincone films and different hybrid structure are listed in Table SI-2 in ESI.<sup>†</sup>

Since gas phase models were used without considering any substrate effect, the starting point of calculation used was diethylzinc and H<sub>2</sub>O to obtain [(OH)ZnC<sub>2</sub>H<sub>5</sub>] species. This was similar to the product formed after the first DEZ pulse on the –OH terminated starting substrate as used experimentally. The primary conclusions obtained from the theoretical calculations can be summed up as follows:

- The formation energy of the first zincone molecule [(HO)Zn(OPhenylOH)] was  $-204.9 \text{ kJ mol}^{-1}$  (steps I and II as detailed in ESI Table SI-2<sup>†</sup>).

Considering this unit of zincone [(HO)Zn(OPhenylOH)] as the unit building block, the formation energies of the successive zincone chains are estimated to be:

- Two units of zincone resulted in a formation energy of  $-205.4 \text{ kJ mol}^{-1}$ . (Steps III and IV as detailed in ESI Table SI-2<sup>†</sup>).

- On the contrary, when a single ZnO moiety is inserted between 2 zincone molecules, formation energy of  $-424.2 \text{ kJ mol}^{-1}$  was obtained (steps III, V, VI and VII as detailed in ESI Table SI-2<sup>†</sup>).

- Insertion of two ZnO moieties between 2 zincone molecules, results in even more exothermic reaction with formation energy of  $-628.4 \text{ kJ mol}^{-1}$ . (steps III, V, VI, VIII, IX, X as detailed in ESI Table SI-2<sup>†</sup>).

Fig. 6 depicts the formation energies of one zincone, two zincone, and two zincone with single and double Zn–O moieties inserted between two. All the energies have been calculated relative to the formation energy of one zincone molecule.

Thus the formation of zincone molecules with ZnO moieties in between was found to be more favorable thermodynamically than only zincone chains confirming our experimental observation that such hybrid structures are more stable than pure zincone molecules.

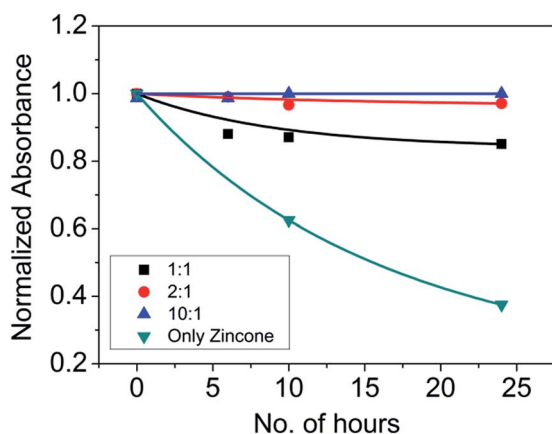


Fig. 5 Variation in the absorbance intensity of Zn–O stretch at  $788 \text{ cm}^{-1}$  position with time with inclusion of 0, 1, 2 and 10 Zn–O moieties between each zincone molecule.

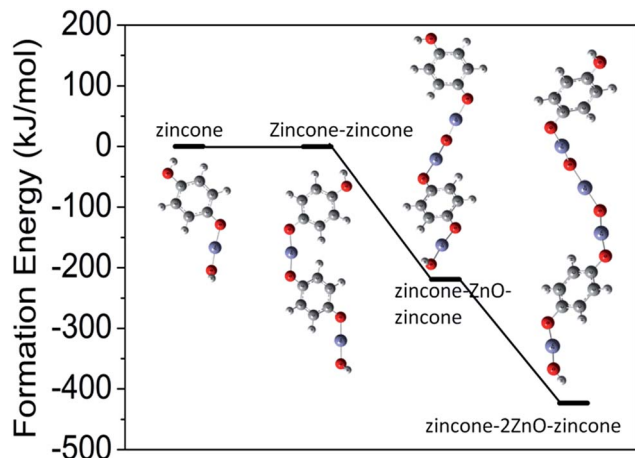


Fig. 6 Formation energies of a single zincone, double zincone, zincone-ZnO-zincone and zincone-2ZnO-zincone molecular chain as calculated from DFT considering single zincone molecule as the unit building block.

## Conclusions

Electrical and chemical stability of hybrid zincone films deposited using diethylzinc and hydroquinone by molecular layer deposition was studied. Experimental observations were supported with DFT based theoretical calculations. The main cause of degradation of the zincone structure was hypothesized and subsequently confirmed to be the breakage of the labile Zn-O bond in the  $[(HO)Zn(OPhenylOH)]_n$  structure. The comparatively longer bond distance of the Zn-O bond in the zincone chain results in the weakness of the bond. Gas phase models were used for the theoretical calculations. Zincone film on complete degradation results in a material closely resembling only hydroquinone. Capping of the zincone films with ZnO and inserting ZnO between zincone monolayers resulted in stable film formations. Thermodynamic energy analysis obtained from DFT calculations confirm the stable nature of alloy films than pure zincone.

## Acknowledgements

This work is supported by the National Centre for Photovoltaic Research and Education (NCPRE) funded by Ministry of New and Renewable Energy of Govt of India.

## Notes and references

- B. H. Lee, B. Yoon, A. I. Abdulagatov, R. A. Hall and S. M. George, *Adv. Funct. Mater.*, 2013, **23**, 532.
- S. M. George, B. H. Lee, B. Yoon, A. I. Abdulagatov and R. A. Hall, *J. Nanosci. Nanotechnol.*, 2011, **11**, 7948.
- B. H. Lee, B. Yoon, V. R. Anderson and S. M. George, *J. Phys. Chem. C*, 2012, **116**, 3250.
- B. H. Lee, M. K. Ryu, S.-Y. Choi, K.-H. Lee, S. Im and M. M. Sung, *J. Am. Chem. Soc.*, 2007, **129**, 16034.
- M. Vähä-Nissi, P. Sundberg, E. Kauppi, T. Hirvikorpi, J. Sievänen, A. Sood, M. Karppinen and A. Harlin, *Thin Solid Films*, 2012, **520**, 6780.
- S. Gupta, S. Seethamraju, P. C. Ramamurthy and G. Madras, *Ind. Eng. Chem. Res.*, 2013, **52**, 4383.
- S.-W. Seo, E. Jung, C. Lim, H. Chae and S. M. Cho, *Thin Solid Films*, 2012, **520**, 6690.
- S. Gupta, S. Sindhu, K. A. Varman, P. C. Ramamurthy and G. Madras, *RSC Adv.*, 2012, **2**, 11536.
- C. R. Kagan, D. B. Mitzi and C. D. Dimitrakopoulos, *Science*, 1999, **286**, 945.
- D. B. Mitzi, *Chem. Mater.*, 2001, **13**, 3283.
- E. Holder, N. Tessler and A. L. Rogach, *J. Mater. Chem.*, 2008, **18**, 1064.
- B. Yoon, B. H. Lee and S. M. George, *J. Phys. Chem. C*, 2012, **116**, 24784.
- M. Karaman, S. E. Kooi and K. K. Gleason, *Chem. Mater.*, 2008, **20**, 2262.
- S. J. Cho, I. S. Bae, H. D. Jeong and J. H. Boo, *Appl. Surf. Sci.*, 2008, **254**, 7817.
- S. Jeong, W.-H. Jang and J. Moon, *Thin Solid Films*, 2004, **466**, 204.
- M. C. Petty, *Langmuir-Blodgett Films-An Introduction*, Cambridge Press, Cambridge University, 1996.
- J. Sánchez-González, J. Ruiz-García and M. J. Gálvez-Ruiz, *J. Colloid Interface Sci.*, 2003, **267**, 286.
- A. Ulman, *An Introduction to Ultrathin Organic Films: From Langmuir-Blodgett to Self-Assembly*, Academic Press, Boston, MA, 1991.
- O. Nilsen, K. Klepper, H. Nielsen and H. Fjellvaåg, *ECS Trans.*, 2008, **16**, 3.
- S. George, A. Dameron, Y. Du, N. M. Adamczyk and S. Davidson, *ECS Trans.*, 2007, **11**, 81.
- S. M. George, *Chem. Rev.*, 2009, **110**, 111.
- D. S. A. A. Dameron, B. B. Burton, S. D. Davidson, A. S. Cavanagh, J. A. Bertrand and S. M. George, *Chem. Mater.*, 2008, **20**, 3315.
- B. Yoon, J. L. O'Patches, D. Seghete, A. S. Cavanagh and S. M. George, *Chem. Vap. Deposition*, 2009, **15**, 112.
- B. H. Lee, V. R. Anderson and S. M. George, *Chem. Vap. Deposition*, 2013, **19**, 204.
- A. I. Abdulagatov, R. A. Hall, J. L. Sutherland, B. H. Lee, A. S. Cavanagh and S. M. George, *Chem. Mater.*, 2012, **24**, 2854.
- L. Ghazaryan, E.-B. Kley, A. Tünnermann and A. Viorica Szeghalmi, *J. Vac. Sci. Technol., A*, 2013, **31**, 01A1491.
- Q. Peng, B. Gong, R. M. VanGundy and G. N. Parsons, *Chem. Mater.*, 2009, **21**, 820.
- B. Yoon, D. Seghete, A. S. Cavanagh and S. M. George, *Chem. Mater.*, 2009, **21**, 5365.
- Y. L. B. Yoon, A. Derk, C. B. Musgrave and S. M. George, *ECS Trans.*, 2011, **33**, 191.
- D. Choudhury, S. K. Sarkar and N. Mahuli, *J. Vac. Sci. Technol., A*, 2015, **33**, 01A115.
- A. Sood, P. Sundberg and M. Karppinen, *Dalton Trans.*, 2013, 3869.

- 32 D. Choudhury and S. K. Sarkar, *Chem. Vap. Deposition*, 2014, **20**, 130.
- 33 M. J. Frisch, G. W. Trucks, H. B. Schlegel, G. E. Scuseria, M. A. Robb, J. R. Cheeseman, J. A. Montgomery Jr, T. Vreven, K. N. Kudin, J. C. Burant, J. M. Millam, S. S. Iyengar, J. Tomasi, V. Barone, B. Mennucci, M. Cossi, G. Scalmani, N. Rega, G. A. Petersson, H. Nakatsuji, M. Hada, M. Ehara, K. Toyota, R. Fukuda, J. Hasegawa, M. Ishida, T. Nakajima, Y. Honda, O. Kitao, H. Nakai, M. Klene, X. Li, J. E. Knox, H. P. Hratchian, J. B. Cross, V. Bakken, C. Adamo, J. Jaramillo, R. Gomperts, R. E. Stratmann, O. Yazyev, A. J. Austin, R. Cammi, C. Pomelli, J. W. Ochterski, P. Y. Ayala, K. Morokuma, G. A. Voth, P. Salvador, J. J. Dannenberg, V. G. Zakrzewski, S. Dapprich, A. D. Daniels, M. C. Strain, O. Farkas, D. K. Malick, A. D. Rabuck, K. Raghavachari, J. B. Foresman, J. V. Ortiz, Q. Cui, A. G. Baboul, S. Clifford, J. Cioslowski, B. B. Stefanov, G. Liu, A. Liashenko, P. Piskorz, I. Komaromi, R. L. Martin, D. J. Fox, T. Keith, M. A. Al-Laham, C. Y. Peng, A. Nanayakkara, M. Challacombe, P. M. W. Gill, B. Johnson, W. Chen, M. W. Wong, C. Gonzalez and J. A. Pople, *R. C. Gaussian 03*, Gaussian, Inc., Wallingford CT, 2004.
- 34 C. Lee, W. Yang and R. G. Parr, *Phys. Rev. B: Condens. Matter Mater. Phys.*, 1988, **37**, 785.
- 35 A. D. Becke, *J. Chem. Phys.*, 1993, **98**, 5648.
- 36 R. Ditchfield, W. J. Hehre and J. A. Pople, *J. Chem. Phys.*, 1971, **54**, 724.
- 37 H. D. Liu, Y. P. Zhao, G. Ramanath, S. P. Murarka and G. C. Wang, *Thin Solid Films*, 2001, **384**, 151.
- 38 H. W. Wilson, *Spectrochim. Acta, Part A*, 1974, **30**, 2141.